

# Orthogonal Subblock Division Multiple Access for OFDM-IM-Based Multi-User VLC Systems

Yungui Nie <sup>1</sup>, Jiamin Chen <sup>1</sup>, Wanli Wen <sup>1</sup>, Min Liu <sup>1</sup>, Xiong Deng <sup>2</sup> and Chen Chen <sup>1,\*</sup> 

<sup>1</sup> School of Microelectronics and Communication Engineering, Chongqing University, Chongqing 400044, China; 202012021020t@cqu.edu.cn (Y.N.); 20183838@cqu.edu.cn (J.C.); wanli\_wen@cqu.edu.cn (W.W.); liumin@cqu.edu.cn (M.L.)

<sup>2</sup> Center for Information Photonics and Communications, Southwest Jiaotong University, Chengdu 610031, China; xiongdeng@swjtu.edu.cn

\* Correspondence: c.chen@cqu.edu.cn

**Abstract:** In this paper, we propose and experimentally demonstrate an orthogonal subblock division multiple access (OSDMA) scheme for orthogonal frequency division multiplexing with index modulation (OFDM-IM)-based multi-user visible light communication (MU-VLC) systems, where both single-mode index modulation (SM-IM) and dual-mode index modulation (DM-IM) are considered. In order to overcome the low-pass frequency response and the light-emitting diodes (LED) nonlinearity issues of practical MU-VLC systems, OSDMA is employed together with discrete Fourier transform spreading (DFT-S) and interleaving. The feasibility and superiority of the proposed scheme have been successfully verified via both simulations and hardware experiments. More specifically, we evaluate and compare the peak-to-average power ratio (PAPR) performance and the bit error rate (BER) performance of OFDM-SM-IM, DFT-S-OFDM-SM-IM, OFDM-DM-IM and DFT-S-OFDM-DM-IM without and with interleaving. Experimental results show that remarkable distance extensions can be achieved by employing DFT spreading and interleaving for both SM-IM and DM-IM in a two-user OSDMA-VLC system.

**Keywords:** visible light communication (VLC); orthogonal frequency division multiplexing (OFDM); index modulation (IM); orthogonal subblock division multiple access (OSDMA)



**Citation:** Nie, Y.; Chen, J.; Wen, W.; Liu, M.; Deng, X.; Chen, C.

Orthogonal Subblock Division Multiple Access for OFDM-IM-Based Multi-User VLC Systems. *Photonics* **2022**, *9*, 373. <https://doi.org/10.3390/photonics9060373>

Received: 6 May 2022

Accepted: 24 May 2022

Published: 25 May 2022

**Publisher's Note:** MDPI stays neutral with regard to jurisdictional claims in published maps and institutional affiliations.



**Copyright:** © 2022 by the authors. Licensee MDPI, Basel, Switzerland. This article is an open access article distributed under the terms and conditions of the Creative Commons Attribution (CC BY) license (<https://creativecommons.org/licenses/by/4.0/>).

## 1. Introduction

In recent years, visible light communication (VLC) using white light-emitting diodes (LEDs) for illumination and communication has been triggering great attention, which has been widely recognized as one of the key enabling technologies of 6G and Internet of Things (IoT) systems [1,2]. VLC has the inherent advantages of abundant unlicensed spectrum resources, anti-electromagnetic interference and simple deployment in comparison to traditional radio frequency (RF) communication [3]. For a practical multi-user VLC (MU-VLC) system based on commercial white LEDs, its performance mainly face two key challenges which are the limited modulation bandwidth and severe nonlinearity of LED [4].

For the bandwidth limitation issue of LEDs, various spectral-efficient modulation techniques and multiple access techniques such as orthogonal frequency division multiplexing (OFDM) and carrierless amplitude and phase (CAP) modulation employing high-order constellations, multiple-input multiple-output (MIMO) and non-orthogonal multiple access (NOMA) can be adopted to achieve high-speed MU-VLC systems [5–8]. In practical orthogonal frequency division multiple access (OFDMA)-based bandlimited MU-VLC systems, the allocated subcarriers of different users might experience different low-pass frequency responses, leading to the degraded overall bit error rate (BER) performance. To address this issue, analog or digital equalization techniques can be applied to flat the system spectrum [9]. Nevertheless, excessive amplification of the power of high-frequency subcarriers might not be feasible due to the limited dynamic range of LEDs [10]. It has been

demonstrated in [11] that interleaved subcarrier multiplexing can be an effective way to ensure that the subcarriers of different users can have comparable signal-to-noise ratio (SNR) performance. For the LED nonlinearity issue, the transmitted signals with reduced peak-to-average power ratios (PAPRs) are less vulnerable to the nonlinearity, and discrete Fourier transform (DFT) spreading can be an efficient approach to significantly reduce the PAPR of OFDM signals [12,13]. Moreover, DFT-spread OFDM (DFT-S-OFDM), which is also known as single-carrier frequency-division multiplexing (SC-FDM), has been widely applied in various scenarios such as local area IMT-A [14] and intensity-modulation/direct-detection (IM/DD) optical interconnects [15].

Recently, OFDM with index modulation (OFDM-IM) has been emerging as a promising technique for 5G and VLC systems, which can transmit additional index bits through subcarrier index selection [16,17]. More specifically, OFDM-IM can be implemented in the single-mode (SM) manner or the dual-mode (DM) manner. For OFDM-SM-IM, only a subset of subcarriers within each subblock are selected and activated to transmit constellation symbols, while the remaining subcarriers are simply left unmodulated. For OFDM-DM-IM, all the subcarriers within each subblock are used to transmit constellation symbols, where the selected subcarriers transmit constellation symbols corresponding to mode 1 while the remaining subcarriers transmit constellation symbols corresponding to mode 2 [18,19]. It has already been shown that OFDM-SM-IM is more power efficient than classical OFDM, which achieves better BER performance than OFDM for relatively low spectral efficiencies. Nevertheless, it is challenging for OFDM-SM-IM to achieve high spectral efficiency due to the existence of unmodulated subcarriers. In contrast, OFDM-DM-IM can achieve high spectral efficiencies, which is able to outperform both classical OFDM and OFDM-SM-IM by carefully designing the dual-mode constellations. Nevertheless, both OFDM-SM-IM and OFDM-DM-IM suffer from high PAPR as classical OFDM, which might not be suitable for practical bandlimited MU-VLC systems with LED nonlinearity. Moreover, differing from classical OFDM which can enable OFDMA for MU-VLC by allocating different users with different subcarriers, subcarrier allocation is not suitable for OFDM-IM as both OFDM-SM-IM and OFDM-DM-IM are performed within a complete subblock. To the best of our knowledge, the efficient application of OFDM-IM techniques in practical bandlimited MU-VLC systems has not yet been considered in the literature.

In this paper, we propose an orthogonal subblock division multiple access (OSDMA) scheme for OFDM-IM-based MU-VLC systems, where both OFDM-SM-IM and OFDM-DM-IM are considered. Moreover, DFT spreading and subcarrier interleaving are employed to address the LED nonlinearity and the low-pass frequency response, respectively. Simulations and experiments have been conducted to verify the feasibility and superiority of the proposed scheme.

## 2. Osdma with DFT-Spreading and Interleaving for Bandlimited MU-VLC

### 2.1. The Review of OFDM-IM

We first review the principle of OFDM-SM-IM and OFDM-DM-IM. It is assumed that the length of each subblock is  $N$  and the OFDM block consists of  $G$  subblocks.

#### 2.1.1. OFDM-SM-IM

For OFDM-SM-IM, the constellation symbols from the constellation set  $\mathcal{M} = [S_1, S_2, \dots, S_M]$  is transmitted on the selected  $k$  subcarriers, while no data is transmitted on the non-selected  $N - k$  subcarriers within each subblock, where  $M$  is the size of  $\mathcal{M}$ . The mapping table of OFDM-SM-IM for  $N = 2$  and  $k = 1$  is given in Table 1. At the receiver side, log-likelihood ratio (LLR) detection is adopted which has been shown to be able to achieve near optimal performance with relatively low computational complexity [16]. We assume that  $y_{\beta}^{\eta}$  ( $\beta = 1, \dots, G; \eta = 1, \dots, N$ ) denote the input signal of the LLR detector, the LLR value with  $\beta$ -th subblock for OFDM-SM-IM signal is shown by

$$\kappa_{\beta}^{\eta} = \ln(k) - \ln(N - k) + \frac{|(y_{\beta}^{\eta})|^2}{N_0} + \ln\left(\sum_{m=1}^M \exp\left(-\frac{1}{N_0}|y_{\beta}^{\eta} - S_m|^2\right)\right), \quad (1)$$

where  $N_0$  denotes the noise power. Hence, the spectral efficiency per subblock for OFDM-SM-IM with  $M$ -ary quadrature amplitude modulation ( $M$ -QAM) constellation is expressed by

$$SE_{\text{OFDM-SM-IM}} = \frac{\lfloor \log_2(C(N, k)) \rfloor + k \log_2(M)}{N}, \quad (2)$$

where  $\lfloor \cdot \rfloor$  and  $C(\cdot, \cdot)$  denote the floor operator and the binomial coefficient, respectively.

**Table 1.** Mapping table of OFDM-SM-IM with  $N = 2$  and  $k = 1$ .

Index Bit	Index	Subblocks
0	1	$[S_m, 0]$
1	2	$[0, S_m]$

### 2.1.2. OFDM-DM-IM

For OFDM-DM-IM, the constellation symbols from the constellation set  $\mathcal{M}_A = [S_1^A, S_2^A, \dots, S_{M_A}^A]$  corresponding to mode 1 is transmitted on the selected  $k$  subcarriers, while the constellation symbols from the constellation set  $\mathcal{M}_B = [S_1^B, S_2^B, \dots, S_{M_B}^B]$  corresponding to mode 2 is transmitted on the non-selected  $N - k$  subcarriers, where  $M_A$  and  $M_B$  are respectively the sizes of  $\mathcal{M}_A$  and  $\mathcal{M}_B$ , and  $\mathcal{M}_A \cap \mathcal{M}_B = \emptyset$ . The mapping table of OFDM-DM-IM for  $N = 2$  and  $k = 1$  is shown in Table 2. Moreover, the LLR value with  $\beta$ -th subblock for OFDM-DM-IM signal is given by

$$\lambda_{\beta}^{\eta} = \ln(k) - \ln(N - k) + \ln\left(\sum_{i=1}^{M_A} \exp\left(-\frac{1}{N_0}|y_{\beta}^{\eta} - S_i^A|^2\right)\right) - \ln\left(\sum_{j=1}^{M_B} \exp\left(-\frac{1}{N_0}|y_{\beta}^{\eta} - S_j^B|^2\right)\right), \quad (3)$$

The spectral efficiency per subblock for OFDM-DM-IM with  $M_A$ -QAM and  $M_B$ -QAM constellations can be obtained as follows

$$SE_{\text{OFDM-DM-IM}} = \frac{b_i + b_c}{N} = \frac{\lfloor \log_2(C(N, k)) \rfloor + k \log_2(M_A) + (N - k) \log_2(M_B)}{N}, \quad (4)$$

**Table 2.** Mapping table of OFDM-DM-IM with  $N = 2$  and  $k = 1$ .

Index Bit	$\mathcal{M}_A$ Index	$\mathcal{M}_B$ Index	Subblocks
0	1	2	$[S_i^A, S_j^B]$
1	2	1	$[S_j^B, S_i^A]$

## 2.2. OSDMA with DFT Spreading and Interleaving

To efficiently apply OFDM-IM techniques in practical bandlimited MU-VLC systems, we proposed an OSDMA scheme with DFT spreading and interleaving. In conventional OFDMA-based MU-VLC, multiple access is achieved via subcarrier allocation among multiple users. However, in the proposed OSDMA-based MU-VLC, multiple access is enabled through subblock allocation. Figure 1a,b show the block diagrams of the transmitter and receiver of the  $K$ -user OSDMA-MU-VLC system with DFT spreading and interleaving,

respectively. Assuming the OSDMA-MU-VLC system consists of totally  $G$  subblocks for valid data transmission and these subblocks are equally allocated to all the  $K$  users, the number of subblocks for each user is  $G/K$ . Hence, letting  $B$  denote the signal bandwidth of the system, the achievable bandwidth of the  $k$ -th user is given by  $B_k = B/K$  ( $k = 1, \dots, K$ ).

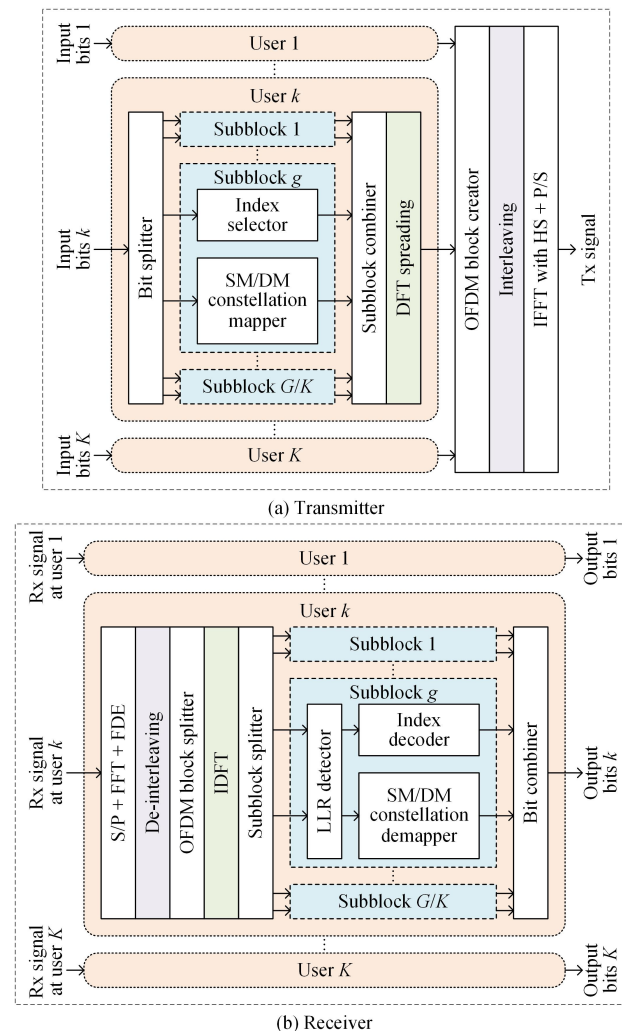


**Figure 1.** Block diagrams of the  $K$ -user OSDMA-MU-VLC system with DFT-spreading and interleaving: (a) transmitter and (b) receiver.

At the transmitter, as shown in Figure 1a, the input bits of the  $k$ -th user are first partitioned into  $G/K$  groups through a bit splitter. In order to generate a subblock with length  $N$ , the input bits of each subblock are further divided into index bits and constellation bits, which are fed into the index selector and the SM/DM constellation mapper, respectively. Subsequently, the  $G/K$  subblocks of the  $k$ -th user are combined by a subblock combiner and DFT spreading is then executed to reduce the PAPR of the signal. After that, all the subblocks for  $K$  users are further concatenated by a OFDM block creator to create a complete OFDM block. Furthermore, interleaving is conducted to mitigate the adverse effect of the low-pass frequency response of the LED. The detailed principle of interleaved subcarrier multiplexing will be discussed in the next subsection. Finally, the transmitted signal is generated after performing inverse fast Fourier transform (IFFT) with Hermitian symmetry (HS) and the parallel-to-serial (P/S) conversion.

At the receiver, as can be seen from Figure 1b, the received signal of the  $k$ -th user is first converted to a parallel signal via serial-to-parallel (S/P). Then, FFT and frequency-domain equalization (FDE) are executed, and de-interleaving is also carried out. Subsequently,

the OFDM block is divided via a OFDM block splitter and inverse DFT (IDFT) is performed accordingly. The  $G/K$  subblocks of the  $k$ -th user can be obtained through a subblock splitter. In each subblock, a low-complexity LLR detector is adopted for signal detection. The index bits and the constellation bits can be recovered through the index decoder and the SM/DM constellation demapper, respectively. The final output bits can be generated by combining the index bits and the constellation bits together via a bit combiner.

### 2.3. Interleaved Subcarrier Multiplexing

In order to address the adverse effect of the low-pass system frequency response on the performance of the  $K$ -user OSDMA-MU-VLC system, interleaved subcarrier multiplexing is performed at the transmitter side. Figure 2a,b illustrate the transmitted spectra without and with interleaving for  $K = 2$ , respectively. For the case without interleaving, the subblocks for user 1 are distributed in the low frequency region while the subblocks for user 2 are distributed in the high frequency region. In contrast, for the case with interleaving, the subcarriers in each subblock are not adjacent each other and the subblocks of each user are distributed over the overall frequency band. Figure 2c,d show the received spectra without and with interleaving for  $K = 2$ . Due to the low-pass frequency response of the system, as can be seen from Figure 2c, the subblocks for user 2 suffer from much more significant power attenuation than that of user 1. As a result, user 1 might achieve a much better BER than that of user 2, leading to a remarkable BER imbalance and hence a degraded overall BER performance of the system. However, when interleaving is performed, as shown in Figure 2d, user 1 and user 2 suffer from a comparable low-pass frequency response. Consequently, user 1 and user 2 might achieve comparable BER performance, which results in a much improved overall BER performance of the system.

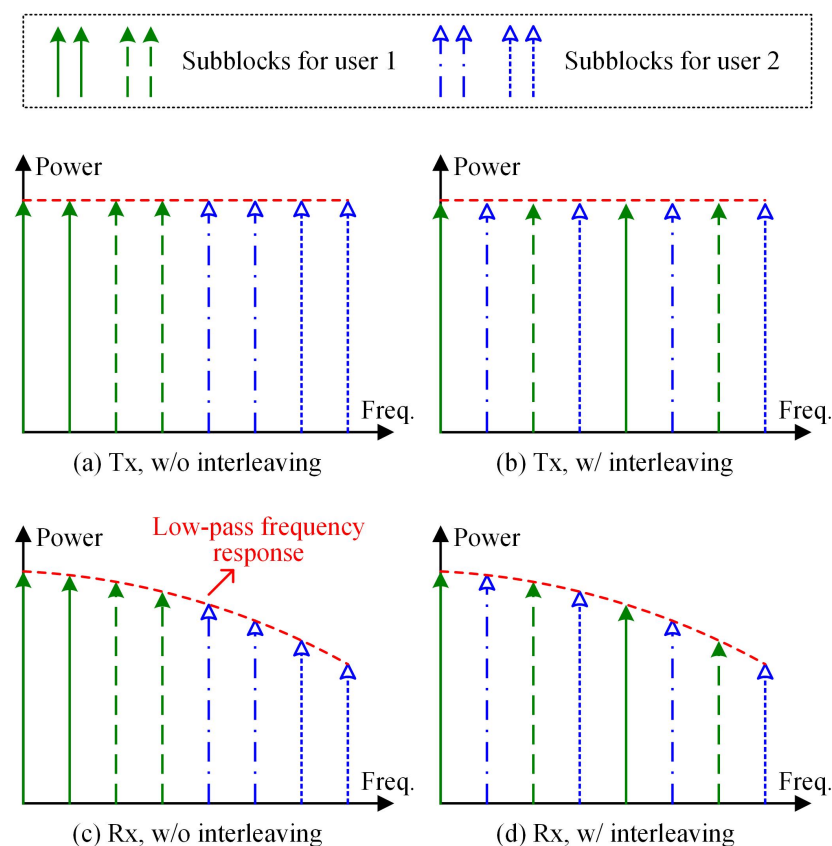


**Figure 2.** Illustration of transmitted spectrum (a) without interleaving and (b) with interleaving, and received spectrum (c) without interleaving and (d) with interleaving.

### 3. Results and Discussions

In this section, we conduct numerical simulations and hardware experiments to evaluate the performance of the proposed OSDMA scheme with DFT spreading and interleaving for OFDM-IM-based MU-VLC systems. Moreover, the following four schemes are considered, including OFDM-SM-IM, DFT-S-OFDM-SM-IM, OFDM-DM-IM and DFT-S-OFDM-DM-IM. In both simulations and experiments, the length of IFFT/FFT is set to 256 and a total of 108 (i.e., 2nd to 109th) subcarriers are utilized to transmit useful signals. Moreover, we consider each subblock with length  $N = 2$  and  $k = 1$  subcarrier is selected via index selection. For all four schemes, a target spectral efficiency of 2.5 bits/s/Hz is considered. Hence, according to (2) and (4), we set  $M = 16$  for OFDM-SM-IM/DFT-S-OFDM-SM-IM and  $M_A = M_B = 4$  for OFDM-DM-IM/DFT-S-OFDM-DM-IM. Specifically, square 16-QAM constellation is adopted for OFDM-SM-IM/DFT-S-OFDM-SM-IM, while the specially-designed circular (7,1)-QAM constellation is considered for OFDM-DM-IM/DFT-S-OFDM-DM-IM [20].

#### 3.1. Simulation Results

In our simulations, we evaluate and compare the PAPR and BER performance of the considered four schemes. It can be clearly seen from Figure 3 that DFT-S-OFDM-SM-IM slightly outperforms OFDM-SM-IM and a PAPR reduction of 0.4 dB is obtained at a probability of  $10^{-3}$ , which might be due to the existence of a large number of unmodulated subcarriers during OFDM modulation. In contrast, a substantial PAPR reduction of 1.9 dB at a probability of  $10^{-3}$  can be achieved by DFT-S-OFDM-DM-IM in comparison to OFDM-DM-IM. As a result, DFT spreading can be considered as an efficient way to reduce the PAPR of OFDM-IM, especially for OFDM-DM-IM. It should be noted that performing interleaved subcarrier multiplexing does not affect the PAPR performance of the above-mentioned schemes.

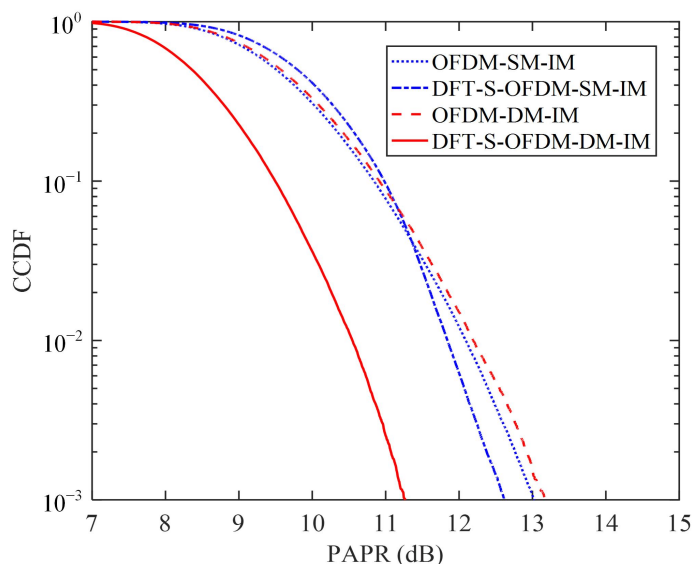
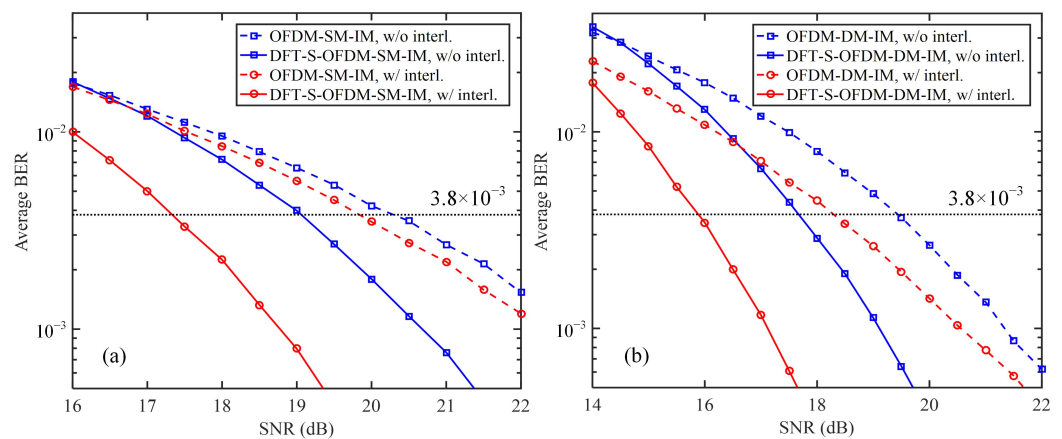


**Figure 3.** PAPR comparison of OFDM-SM-IM, DFT-S-OFDM-SM-IM, OFDM-DM-IM, and DFT-S-OFDM-DM-IM.

Figure 4a shows the simulation BER versus signal-to-noise ratio (SNR) for OFDM-SM-IM and DFT-S-OFDM-SM-IM without and with interleaving over a low-pass VLC channel, where the noise is modeled as the additive white Gaussian noise (AWGN) and the adopted low-pass frequency response is measured from the experimental VLC system which can be found in Section 3.2. As we can see, OFDM-SM-IM with interleaving slightly outperforms OFDM-SM-IM without interleaving by an SNR gain of 0.5 dB at the 7% forward error correction (FEC) coding limit of  $\text{BER} = 3.8 \times 10^{-3}$ . Moreover, an SNR gain of 1.2 dB can be obtained by DFT-S-OFDM-SM-IM without interleaving in comparison to OFDM-SM-



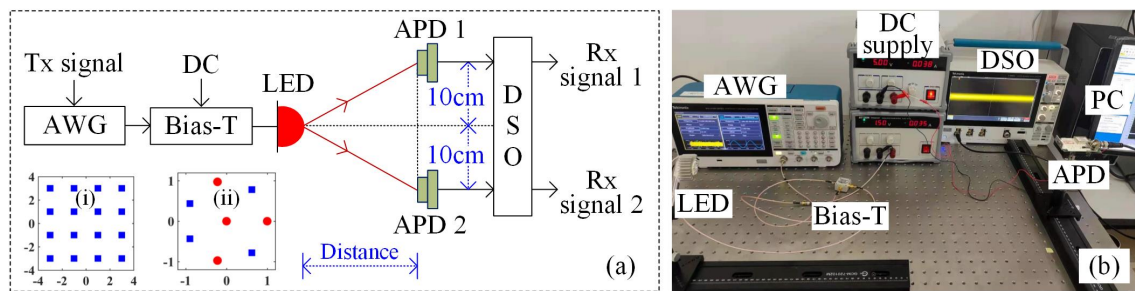
IM without interleaving. It is clearly to see that the combination of DFT spreading and interleaving can lead to a significant 3-dB SNR gain for OFDM-SM-IM. Figure 4b depicts the simulation BER versus SNR for OFDM-DM-IM and DFT-S-OFDM-DM-IM without and with interleaving over the low-pass VLC channel. It can also be observed that DFT-S-OFDM-DM-IM with interleaving outperforms DFT-S-OFDM-DM-IM without interleaving, OFDM-DM-IM with interleaving and OFDM-DM-IM without interleaving by SNRs gain of 1.8, 2.4 and 3.5 dB, respectively.



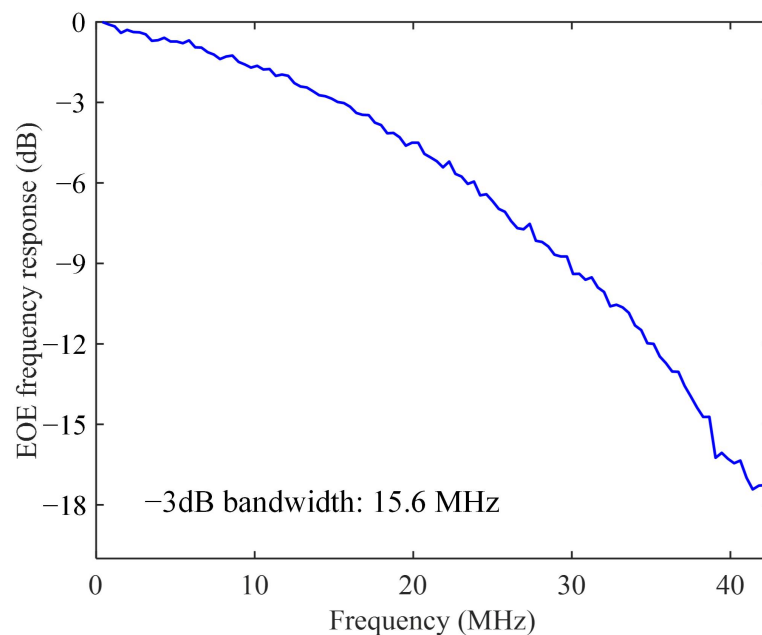
**Figure 4.** Simulation BER vs. SNR for (a) OFDM-SM-IM and DFT-S-OFDM-SM-IM and (b) OFDM-DM-IM and DFT-S-OFDM-DM-IM without and with interleaving over the low-pass VLC channel (w/o: without, w/: with, interl.: interleaving).

### 3.2. Experimental Results

We further experimentally investigate the performance of the OSDMA-MU-VLC system. The experimental setup of a two-user OSDMA-VLC system is shown in Figure 5a, where the transmitted signal is firstly generated offline by MATLAB and then sent to an arbitrary waveform generator (AWG, Tektronix AFG31102) with a sampling rate of 100 MSa/s. As a result, the bandwidth of the AWG output signal is 42 MHz and the data rate is 105 Mbits/s for all the schemes. The peak-to-peak voltage ( $V_{pp}$ ) of the AWG output signal is 3 V. After that, the AWG output signal is combined with a 35-mA DC bias current via a bias-tee (bias-T, Mini-Circuits ZFBT-6GW+) to drive the infrared LED. At the receiver side, each user is equipped with an avalanche photo-diode (APD, Hamamatsu C12702-12) to detect the optical signal and perform optical-to-electrical (O/E) conversion. It can be seen from Figure 5a the two users have the same vertical offset of 10 cm from the center of the LED while the horizontal distance is in the range between 40 to 80 cm. Subsequently, the received electrical signal of each user is captured by a digital storage oscilloscope (DSO, Tektronix MDO32) with a sampling rate of 500 MSa/s, which is further processed offline by MATLAB. Moreover, the square 16-QAM constellation for OFDM-SM-IM/DFT-S-OFDM-SM-IM and the circular (7,1)-QAM constellation for OFDM-DM-IM/DFT-S-OFDM-DM-IM are shown in the insets (i) and (ii) of Figure 5a, respectively. The photo of the overall experimental system is given in Figure 5b. Figure 6 shows the measured frequency response of the VLC system which is obtained by using the OFDM-based channel estimation method. As we can see, the system exhibits a typical low-pass characteristic and the -3dB bandwidth is 15.6 MHz.



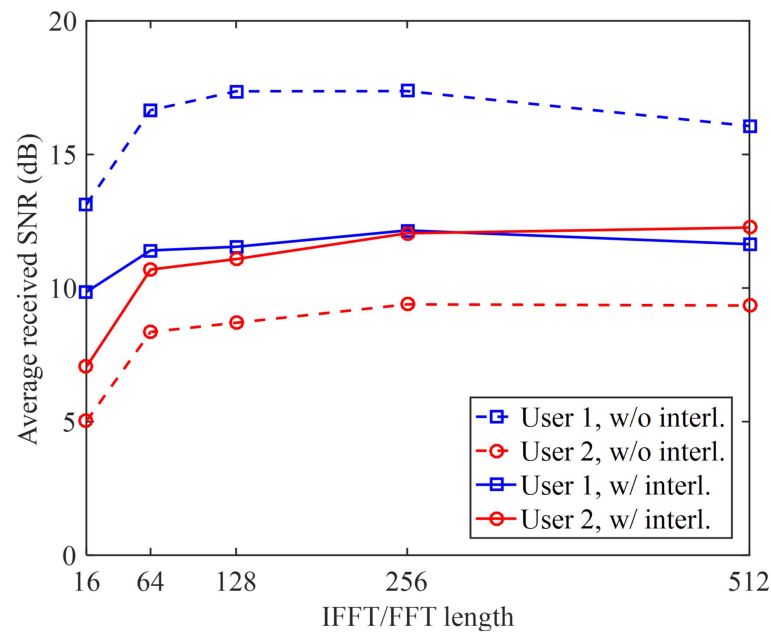
**Figure 5.** (a) Experimental setup of a two-user OSDMA-VLC system and (b) the photo of the experimental system.



**Figure 6.** EOE frequency response of the experimental VLC system.

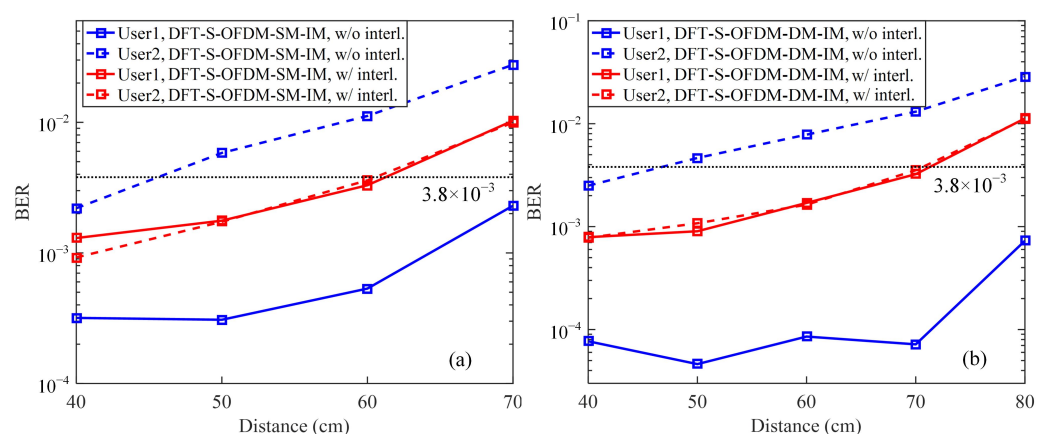
Figure 7 shows the measured average received SNR of each user without and with interleaving versus the length of IFFT/FFT, where the transmission distance is 60 cm. As we can observe, as the length of IFFT/FFT is increased from 16 to 256, the average received SNR of each user is gradually increased. Moreover, the average received SNR of each user becomes stable when the length of IFFT/FFT is larger than 256. For the case without interleaving, the average received SNRs of 17.4 and 9.4 dB are obtained by user 1 and user 2, respectively, when the length IFFT/FFT is 256. Hence, there exists an SNR difference of up to 8 dB for two users which is mainly caused by the low-pass frequency response of the bandlimited VLC system. In contrast, for the case with interleaving, the two users can achieve comparable SNRs when the length of IFFT/FFT reaches 256, indicating that interleaved subcarrier multiplexing is an efficient approach to mitigate user SNR unbalance. In our following experiments, the length of IFFT/FFT is fixed as 256.





**Figure 7.** Average received SNR vs. IFFT/FFT length of the DFT-S-OFDM signal (w/o: without, w/: with, interl.: interleaving).

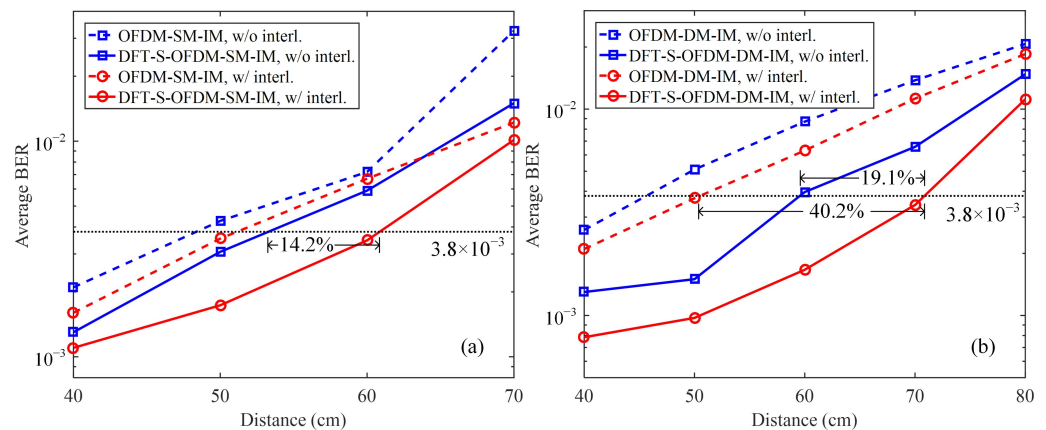
Figure 8a,b show the measured BER versus the transmission distance for DFT-S-OFDM-SM-IM and DFT-S-OFDM-DM-IM, respectively. For DFT-S-OFDM-SM-IM without and with interleaving, as shown in Figure 8a, the BERs of all schemes can reach the 7% FEC coding limit of  $3.8 \times 10^{-3}$  within the distance range of 40 to 70 cm. It can be clearly seen that the BERs of the two users for DFT-S-OFDM-SM-IM without interleaving are quite different and the maximum distances that can be transmitted by user 1 and user 2 below  $\text{BER} = 3.8 \times 10^{-3}$  are over 70 cm and about 45.3 cm, respectively. In contrast, for DFT-S-OFDM-SM-IM with interleaving, the two users can achieve comparable BERs and nearly the same maximum distances of about 61 cm can be achieved. The same conclusion can be found for DFT-S-OFDM-DM-IM, as shown in Figure 8b, which agrees well with the findings in Figure 6.



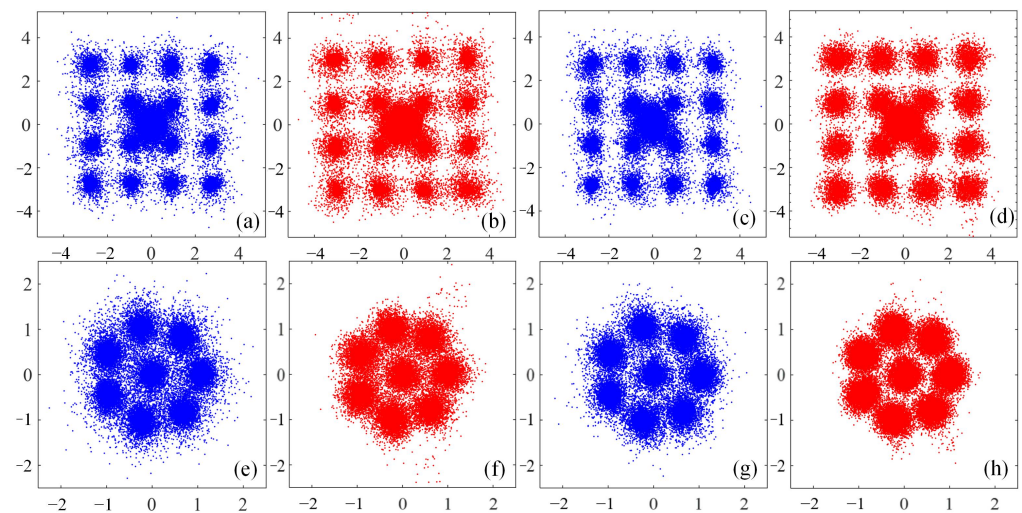
**Figure 8.** Measured BER vs. distance for (a) DFT-S-OFDM-SM-IM without and with interleaving and (b) DFT-S-OFDM-DM-IM without and with interleaving (w/o: without, w/: with, interl.: interleaving).

Figure 9 shows the measured average BER versus transmission distance for different schemes. As shown in Figure 9a, the maximum distance below  $\text{BER} = 3.8 \times 10^{-3}$  that can be achieved by OFDM-SM-IM without interleaving is 48.3 cm, which is slightly increased to 53.2 cm when interleaving is performed. The maximum distances below  $\text{BER} = 3.8 \times 10^{-3}$  for DFT-S-OFDM-SM-IM without and with interleaving are 51.2 and 60.8 cm, respectively.

Hence, an distance extension of 14.24% is obtained by DFT-S-OFDM-SM-IM with interleaving in comparison to that without interleaving. Moreover, it can be seen from Figure 9b that a significant distance extension of 40.2% is obtained for DFT-S-OFDM-DM-IM with interleaving when compared with OFDM-DM-IM with interleaving, while DFT-S-OFDM-DM-IM with interleaving also achieves a distance extension of 19.1% in comparison to that without interleaving. The results shown in Figure 9a,b indicate that it is beneficial to perform DFT spreading and interleaving in OSDMA-based practical MU-VLC systems. In addition, the corresponding received constellation diagrams are depicted in Figure 10a–h.



**Figure 9.** Average BER vs. distance for (a) OFDM-SM-IM and DFT-S-OFDM-SM-IM without and with interleaving and (b) OFDM-DM-IM and DFT-S-OFDM-DM-IM without and with interleaving (w/o: without, w/: with, interl.: interleaving).



**Figure 10.** The received constellation diagrams for: (a) OFDM-SM-IM, 16QAM, 50 cm, without interleaving, (b) DFT-S-OFDM-SM-IM, 16QAM, 50 cm, without interleaving, (c) OFDM-SM-IM, 16QAM, 50 cm, with interleaving, (d) DFT-S-OFDM-SM-IM, 16QAM, 50 cm, with interleaving, (e) OFDM-DM-IM, circular (7,1)QAM, 60 cm, without interleaving, (f) DFT-S-OFDM-DM-IM, circular (7,1)QAM, 60 cm, without interleaving, (g) OFDM-DM-IM, circular (7,1)QAM, 60 cm, with interleaving, and (h) DFT-S-OFDM-DM-IM, circular (7,1)QAM, 60 cm, with interleaving.

#### 4. Conclusions

In this paper, a novel OSDMA scheme is proposed and investigated for OFDM-IM-based MU-VLC systems. Moreover, DFT spreading and interleaved subcarrier multiplexing are further introduced to address both the low-pass frequency response and the LED nonlinearity issues of practical MU-VLC systems. It has been verified through numerical simulations and hardware experiments that both OFDM-SM-IM and OFDM-DM-IM can

achieve substantial performance improvements when DFT spreading and interleaving are performed. More specifically, simulation results show that more than 3-dB SNR gains can be obtained when DFT spreading and interleaving are performed for both OFDM-SM-IM and OFDM-DM-IM over a low-pass VLC channel, while experimental results demonstrate that substantial distance extensions of 40.2% and 19.1% can be achieved by DFT-S-OFDM-DM-IM with interleaving compared with OFDM-DM-IM with interleaving and DFT-S-OFDM-DM-IM without interleaving, respectively. Therefore, OSDMA with DFT spreading and interleaving can be a promising candidate for practical high-speed MU-VLC systems.

**Author Contributions:** Formal analysis, W.W., M.L., X.D. and C.C.; funding acquisition, C.C.; investigation, Y.N. and J.C.; methodology, J.C.; project administration, C.C.; resources, X.D.; software, J.C.; supervision, M.L. and C.C.; validation, Y.N.; writing – original draft, Y.N.; writing – review & editing, W.W., X.D. and C.C. All authors have read and agreed to the published version of the manuscript.

**Funding:** This research was funded by the National Natural Science Foundation of China (61901065 and 62001174), the Natural Science Foundation of Chongqing (cstc2021jcyj-msxmX0480), and the Fundamental Research Funds for the Central Universities (2021CDJQY-013).

**Institutional Review Board Statement:** Not applicable.

**Informed Consent Statement:** Not applicable.

**Data Availability Statement:** Not applicable.

**Acknowledgments:** The authors would like to thank the anonymous reviewers for their valuable comments and suggestions.

**Conflicts of Interest:** The authors declare no conflict of interest.

## References

1. Chi, N.; Zhou, Y.; Wei, Y.; Hu, F. Visible light communication in 6G: Advances, challenges, and prospects. *IEEE Veh. Technol. Mag.* **2020**, *15*, 93–102.
2. Chen, C.; Fu, S.; Jian, X.; Liu, M.; Deng, X.; Ding, Z.G. NOMA for energy-efficient LiFi-enabled bidirectional IoT communication. *IEEE Trans. Commun.* **2021**, *69*, 1693–1706.
3. Komine, T.; Nakagawa, M. Fundamental analysis for visible-light communication system using LED lights. *IEEE Trans. Consum. Electron.* **2004**, *50*, 100–107.
4. Deng, X.; Mardanikorani, S.; Wu, Y.; Arulandu, K.; Chen, B.; Khalid, A.M.; Linnartz, J.P. Mitigating LED nonlinearity to enhance visible light communications. *IEEE Trans. Commun.* **2018**, *66*, 5593–5607.
5. Chen, C.; Zhong, W.D.; Yang, H.L.; Du, P.F. On the performance of MIMO-NOMA based visible light communication systems. *IEEE Photonics Technol. Lett.* **2018**, *30*, 307–310.
6. Nie, Y.G.; Zhang, W.; Yang, Y.B.; Deng, X.; Liu, M.; Chen, C. Pairwise coded mCAP with chaotic dual-mode index modulation for secure bandlimited VLC systems. *Photonics* **2022**, *9*, 141.
7. Elgala, H.; Mesleh, R.; Haas, H. Indoor broadcasting via white LEDs and OFDM. *IEEE Trans. Consum. Electron.* **2009**, *55*, 1127–1134.
8. Lin, B.; Zhang, K.; Tian, Y.; Chen, Y.; Tang, X.; Zhang, M.; Wu, Y.; Li, H. Non-orthogonal multiple access for visible light communications. In Proceedings of the Asia Communications and Photonics Conference, Guangzhou, China, 10–13 November 2017; paper Su2A.22.
9. Li, J.F.; Huang, Z.T.; Liu, X.S.; Ji, Y.F. Hybrid time-frequency domain equalization for LED nonlinearity mitigation in OFDM-based VLC systems. *Opt. Express* **2015**, *25*, 611–619.
10. Chen, C.; Nie, Y.G.; Liu, M.; Du, Y.F.; Liu, R.S.; Wei, Z.X.; Fu, H.Y. Digital pre-equalization for OFDM-based VLC systems: Centralized or distributed? *IEEE Photonics Technol. Lett.* **2021**, *33*, 1081–1084.
11. Chen, C.; Tang, Y.R.; Cai, Y.P.; Liu, M. Fairness-aware hybrid NOMA/OFDMA for bandlimited multi-user VLC systems. *Opt. Express* **2021**, *29*, 42265–42275.
12. Nisar, M.D.; Nottensteiner, H.; Hindelang, T. On performance limits of DFT spread OFDM systems. In Proceedings of the 16th IST Mobile and Wireless Communications Summit, Budapest, Hungary, 1–5 July 2007; pp. 1–4.
13. Ahmed, F.; Nie, Y.G.; Chen, C.; Liu, M.; Du, P.F.; Alphones, A. DFT-spread OFDM with quadrature index modulation for practical VLC systems. *Opt. Express* **2021**, *29*, 33027–33036.
14. Berardinelli, G.; de Temino, L.A.M.; Frattasi, S.; Rahman, M.I.; Mogensen, P. OFDMA vs. SC-FDMA: Performance comparison in local area IMT-A scenarios. *IEEE Wirel. Commun.* **2008**, *15*, 64–72.

15. Zhou, J.; Qiao, Y.J.; Yu, J.J.; Shi, J.Y.; Cheng, Q.X.; Tang, X.Z.; Guo, M.G. Interleaved single-carrier frequency-division multiplexing for optical interconnects. *Opt. Express*. **2017**, *25*, 10586–10596.
16. Basar, E. Index modulation techniques for 5G wireless networks. *IEEE Commun. Mag.* **2016**, *54*, 168–175.
17. Chen, C.; Deng, X.; Yang, Y.B.; Du, P.F.; Yang, H.L.; Zhong, W.D. Experimental demonstration of optical OFDM with subcarrier index modulation for IM/DD VLC. In Proceedings of the Asia Communications and Photonics Conference (ACP), Chengdu, China, 2–5 November 2019; paper M4A.40.
18. Mao, T.Q.; Wang, Z.C.; Wang, Q.; Chen, S.; Hanzo, L. Dual-mode index modulation aided OFDM. *IEEE Access*. **2017**, *5*, 50–60.
19. Mao, T.Q.; Jiang, R.; Bai, R.W. Optical dual-mode index modulation aided OFDM for visible light communications. *Opt. Commun.* **2017**, *391*, 37–41.
20. Zhao, J.; Qin, C.; Zhang, M.; Chi, N. Investigation on performance of special-shaped 8-quadrature amplitude modulation constellations applied in visible light communication. *Photon. Res.* **2016**, *4*, 249–256.